

Genuine tripartite entanglement in the non-interacting Fermi gas

T. Vértesi

*Institute of Nuclear Research of the Hungarian Academy of Sciences,
H-4001 Debrecen, P.O. Box 51, Hungary*

(Dated: October 7, 2018)

We study genuine tripartite entanglement shared among the spins of three localized fermions in the non-interacting Fermi gas at zero temperature. Firstly, we prove analytically with the aid of entanglement witnesses that in a particular configuration the three fermions are genuinely tripartite entangled. Then various three-fermion configurations are investigated in order to quantify and calculate numerically the amount of genuine tripartite entanglement present in the system. Further we give a lower and an upper limit to the maximum diameter of the three-fermion configuration below which genuine tripartite entanglement exists and find that this distance is comparable with the maximum separation between two entangled fermions. The upper and lower limit turn to be very close to each other indicating that the applied witness operator is well suited to reveal genuine tripartite entanglement in the collection of non-interacting fermions.

PACS numbers: 03.65.Ud, 03.67.Mn, 71.10.Ca

I. INTRODUCTION

Entanglement is in the heart of quantum mechanics and of great importance in quantum information theory. Two entangled particles already offer a valuable resource to perform several practical tasks such as quantum teleportation, quantum cryptography or quantum computation [1]. However, the multipartite setting due to the much richer structure suggests many new possibilities and phenomena over the bipartite case. Indeed, multipartite states may contradict local realistic models in a qualitatively different and stronger way [2]. Moreover, this feature allows to implement novel quantum information processing tasks such as quantum computation based on cluster states [3], entanglement enhanced measurements [4], quantum communication without a common reference frame [5] and open-destination teleportation [6].

Though the characterization of multipartite entanglement is studied in great depth [7, 8], still rarely investigated in solid state systems (see [9] and references therein), however, it definitely plays an essential role in quantum phase transitions [10, 11] and might well be a key ingredient to unresolved problems in physics such as high temperature superconductivity [12]. In this article we investigate genuine multipartite entanglement shared among the spins of three fermions in the Fermi gas of non-interacting particles at zero temperature (degenerate Fermi gas) following the work of Refs. [13, 14]. We apply an entanglement witness developed in Ref. [9] (and also appeared in Ref. [15]) in order to reveal genuine tripartite quantum correlations in the collection of fermions and using the approach in Ref. [16] we also characterize quantitatively the amount of it.

The article is organized as follows: In Sec. II according to Refs. [13, 14] we present the three-spin reduced density matrix of the degenerate Fermi gas, and show by analytical means (extending the related results of Ref. [14]) that both *GHZ*-type and *W*-type witnesses are unable

to detect genuine tripartite entanglement (GTE) among the spins of three localized fermions. On the other, we demonstrate that for specific configurations of the three fermions the GTE witness of Ref. [9] is capable to signal GTE both for the two- and three-dimensional (2D and 3D) degenerate Fermi gases. In Sec. III on the basis of this witness a formula is constructed to the lower bound of the generalized robustness (E_R) of genuine tripartite entanglement. With the aid of this formula in Sec. IV we quantify numerically genuine tripartite quantum correlations for various arrangements of the three particles. In Sec. V we determine lower and upper bounds to the GTE distance (i.e., to the largest diameter of the three-fermion configuration below which GTE is still present in the system) both in the 2D and 3D degenerate Fermi gases. The paper concludes in Sec. VI with a brief summary of the results obtained and discusses possible schemes to extract GTE from the system.

II. ANALYSIS OF THE DENSITY MATRIX FOR THREE FERMIONS

A. Three-spin reduced density matrix

Consider a system of N non-interacting fermions in a box with volume V . At zero temperature the ground state of the system is $|\phi_0\rangle = \prod_k^{k_F} \hat{c}_{k,\sigma}^\dagger |vac\rangle$, where $k_F = (3\pi^2 N/V)^{1/3}$ is the Fermi momentum and $|vac\rangle$ denotes the vacuum state. From the ground state of the system $|\phi_0\rangle$ one obtains the three-spin reduced density matrix (up to normalization) between the three fermions localized at positions \mathbf{r} , \mathbf{r}' , and \mathbf{r}'' ,

$$\rho_3(s, s', s''; t, t', t'') = \langle \phi_0 | \hat{\psi}_t^\dagger(\mathbf{r}) \hat{\psi}_{t'}^\dagger(\mathbf{r}') \hat{\psi}_{t''}^\dagger(\mathbf{r}'') \hat{\psi}_{s''}(\mathbf{r}'') \hat{\psi}_{s'}(\mathbf{r}') \hat{\psi}_s(\mathbf{r}) | \phi_0 \rangle, \quad (1)$$

where $\hat{\psi}_s(\mathbf{r})$, $\hat{\psi}_s^\dagger(\mathbf{r})$ are field annihilation/creation operators for a particle with spin s located at position \mathbf{r} sat-

isfying $\{\hat{\psi}_s(\mathbf{r}), \hat{\psi}_s^\dagger(\mathbf{r}')\} = \delta_{s,s'}\delta(\mathbf{r} - \mathbf{r}')$. The justification, that the above matrix elements indeed describe three-qubit quantum states is discussed in the Appendix of Ref [18]. Following Refs. [13, 14] the explicit formula for the three-spin reduced density matrix ρ_3 is given by

$$\rho_3 = (1-p)\frac{\mathbb{I}_8}{8} + p_{12}|\Psi_{12}^-\rangle\langle\Psi_{12}^-| \otimes \frac{\mathbb{I}_4}{2} + p_{13}|\Psi_{13}^-\rangle\langle\Psi_{13}^-| \otimes \frac{\mathbb{I}_4}{2} + p_{23}|\Psi_{23}^-\rangle\langle\Psi_{23}^-| \otimes \frac{\mathbb{I}_4}{2}, \quad (2)$$

where $p = p_{12} + p_{13} + p_{23}$ and \mathbb{I}_n denotes the $n \times n$ identity matrix. Further, $\Psi_{ij}^- = (|\uparrow\downarrow\rangle - |\downarrow\uparrow\rangle)/\sqrt{2}$ is the singlet state of the pair ij in the orthonormal basis $\{|\uparrow\rangle, |\downarrow\rangle\}$. The value p_{ij} depends only on the relative distance between the three fermions and can be written explicitly for the fermion pair ij as [14]

$$p_{ij} = \frac{-f_{ij}^2 + f_{ij}f_{ik}f_{jk}}{-2 + f_{ij}^2 + f_{ik}^2 + f_{jk}^2 - f_{ij}f_{ik}f_{jk}}, \quad (3)$$

where the analytic form of f_{ij} depends on the spatial dimension of the system, that is we may write

$$\begin{aligned} f_{ij}^{2D} &= 2J_1(k_F r_{ij})/k_F r_{ij} \\ f_{ij}^{3D} &= 3j_1(k_F r_{ij})/k_F r_{ij} \end{aligned} \quad (4)$$

in the case of the two- and three-dimensional Fermi gases [19]. In the above formulae j_1 and J_1 denote the spherical and the first order Bessel function of the first kind, respectively.

Actually, owing to the collective $SU(2)$ rotational symmetry of the model Hamiltonian of non-interacting fermions, many matrix elements of ρ_3 in (2) are forced to be zero. Explicitly, the states which are invariant under collective $SU(2)$ rotation of the three qubits are the three-qubit Werner states [20], and they can be given in the form [20]

$$\rho = \sum_{k=+,0,1,2,3} \frac{r_k}{4} R_k, \quad (5)$$

where R_k are certain linear combinations of permutation operators and $r_k(\rho) = \text{Tr}(\rho R_k)$. Using the definitions for R_k from Ref. [20] and the explicit form of the state ρ_3 from (2), we are able to calculate the parameters r_k for the three-spin reduced density matrix ρ_3 , which read as follows

$$\begin{aligned} r_+ &= \frac{1-p}{2} \\ r_0 &= \frac{1+p}{2} \\ r_1 &= \frac{p_{12} + p_{13} - 2p_{23}}{2} \\ r_2 &= \frac{3}{2\sqrt{3}}(p_{13} - p_{12}) \\ r_3 &= 0. \end{aligned} \quad (6)$$

B. Possible range of parameters p_{ij}

According to the Lemma 2 of Ref. [20] ρ in (5) is a density matrix only if $r_+, r_0 \geq 0$. These inequalities imply for the state ρ_3 by the virtue of (6) that p lies in the interval

$$-1 \leq p \leq +1. \quad (7)$$

Let us observe in (4) that $|f_{ij}| \leq 1$ both for the 2D and 3D Fermi gases. This fact together with the bound to p in (7) and also the definition $p = p_{12} + p_{13} + p_{23}$, after some algebraic manipulations (which are not detailed here), lead to the bounds

$$-1 \leq p_{ij} \leq 1 \quad (8)$$

for the three different fermion pairs $ij = 12, 13, 23$. Thus, the parameters p_{ij} appearing in state ρ_3 are limited by the values ± 1 .

Let us introduce the class of biseparable three-qubit states B , i.e., the states

$$\rho = \sum_i p_i |\psi_i\rangle\langle\psi_i|, \quad (9)$$

which can be expressed as a convex sum of projectors onto product and bipartite entangled vectors [7]. In definition (9) the pure states $|\psi_i\rangle$ are separable on the Hilbert-space of three qubits 1, 2, 3 with respect to one of the three bipartitions 1|23, 12|3 or 13|2 and $p_i \geq 0$ adding up to 1. We say that a general three-qubit state is genuine tripartite entangled when it is not in the class of biseparable states B , that is they cannot be constructed by mixing pure states containing bipartite entanglement at most. Clearly, if p_{ij} in (2) was positive for each of the three different pairs (whose sum p is upper bounded by +1 according to (7)), then ρ_3 should define a biseparable state.

Note, that the bound to p_{ij} 's in (8) may not be tight, therefore it is not evident whether p_{ij} can take up negative values at all. However, by arranging the three fermions in a particular geometry, we demonstrate that p_{ij} may take the value $-1/3$ as well: Taking the first and second derivatives of the functions $f_{ij}(k_F r)$ (defined for both the 2D and 3D Fermi gases under equations (4)) with respect to $x = k_F r$, we observe that in the limit $x \rightarrow 0$ they behave as

$$\lim_{x \rightarrow 0} f_{ij}(x) = 1, \quad \lim_{x \rightarrow 0} f'_{ij}(x) = 0, \quad \lim_{x \rightarrow 0} f''_{ij}(x) \neq 0. \quad (10)$$

Now let us place the three particles on a line so that particle 2 would lie just at the midpoint between particle 1 and particle 3, and let the relative distance between these outer particles tends to zero. Actually, in the limit $x \rightarrow 0$, p_{ij} in (3) can be given explicitly by applying l'Hospital's rule twice and by taking account the limiting values (10). As a result we obtain

$$p_{12} = p_{23} = 2/3, \quad p_{13} = -1/3 \quad (11)$$

both for the 2D and 3D Fermi gases.

In the next two subsections we propose witness operators in order to reveal GTE in the degenerate Fermi systems. An observable which is well suited for signaling genuine tripartite quantum correlations in Heisenberg spin lattices [9] turns out to detect GTE in the degenerate Fermi gas as well.

C. Generalized GHZ and W witnesses

For deciding whether the state ρ_3 with the explicit parameters $p_{12} = p_{23} = 2/3$, $p_{13} = -1/3$ in (11) is genuine tripartite entangled, we will use entanglement witnesses. A witness of genuine tripartite entanglement is an observable Π with a positive mean value on all biseparable states so a negative expectation value $\text{Tr}(\rho\Pi)$ guarantees that the state ρ carries genuine tripartite entanglement [21]. Thus a witness operator which separates genuine tripartite entangled states from the biseparable set B (defined by equation (9)) can be given in the form [22]

$$W_\psi = \Lambda \mathbb{I}_8 - |\psi\rangle\langle\psi|, \quad (12)$$

where

$$\Lambda = \max_{|\phi\rangle \in B} |\langle\phi|\psi\rangle|^2. \quad (13)$$

A simple method has been found in Ref. [22] to determine Λ for any pure genuine tripartite entangled state $|\psi\rangle$. In particular, let $|\psi\rangle$ be the GHZ -like and the W -like state [23], which are respectively

$$\begin{aligned} |GHZ(\alpha)\rangle &= \frac{|\mathbf{n}_1, \mathbf{n}_2, \mathbf{n}_3\rangle + e^{i\alpha}|\mathbf{n}_1, -\mathbf{n}_2, -\mathbf{n}_3\rangle}{\sqrt{2}} \\ |W(\beta, \gamma)\rangle &= \frac{|\mathbf{n}_1, \mathbf{n}_2, -\mathbf{n}_3\rangle + e^{i\beta}|\mathbf{n}_1, -\mathbf{n}_2, \mathbf{n}_3\rangle + e^{i\gamma}|\mathbf{n}_1, \mathbf{n}_2, \mathbf{n}_3\rangle}{\sqrt{3}}, \end{aligned} \quad (14)$$

where $\{\mathbf{n}_i, -\mathbf{n}_i\}$ denotes an arbitrary local orthonormal basis in the Hilbert space of qubit i . Note, that for the original GHZ state the phase $\alpha = 0$ and for the original W state the phases $\beta = \gamma = 0$, and the corresponding parameters Λ appearing in the witness operator (12) are $1/2$ and $2/3$, respectively [7]. The states (14), however, can be transferred to the original ones by local unitary operations, which leave the parameters Λ unchanged, that is we have the witness operators

$$\begin{aligned} W_{GHZ(\alpha)} &= \frac{1}{2}\mathbb{I}_8 - |GHZ(\alpha)\rangle\langle GHZ(\alpha)| \\ W_{W(\beta, \gamma)} &= \frac{2}{3}\mathbb{I}_8 - |W(\beta, \gamma)\rangle\langle W(\beta, \gamma)| \end{aligned} \quad (15)$$

for the GHZ - and W -like states, respectively.

Lunkes et al. [14] applying these witness operators for the special case $\alpha = \beta = \gamma = 0$ and $|\mathbf{n}_i\rangle = |\uparrow\rangle$, $i = 1, 2, 3$ established that neither $\text{Tr}(\rho_3 W_{GHZ})$ nor $\text{Tr}(\rho_3 W_W)$ can become negative in the permitted range of parameters

p_{ij} , $ij = 12, 13, 23$, hence no GTE could be revealed in the three-spin reduced density matrix ρ_3 by the application of these witnesses.

We confirm and extend this result by generalizing the GHZ and W witnesses to the form (15) with the corresponding values $\alpha, \beta, \gamma \in [0, 2\pi]$ and with the arbitrary local bases $|\mathbf{n}_i\rangle = \cos(\theta_i/2)|\uparrow\rangle + e^{i\phi_i}\sin(\theta_i/2)|\downarrow\rangle$, $i = 1, 2, 3$. Then the trace of $\rho_3\Pi$, where Π denotes either $W_{GHZ(\alpha)}$ or $W_{W(\beta, \gamma)}$ and ρ_3 is the state (2), is a linear combination of the trigonometric functions cosine/sine with arguments θ_i, ϕ_i , $i = 1, 2, 3$. Owing to convexity arguments $\text{Tr}(\rho_3\Pi)$ can be extremal only if $p_{ij} \in \{+1, -1\}$, $ij = 12, 13, 23$ in the permitted range (8) and $\theta_i, \phi_i \in \{0, \pi/2, \pi, 3\pi/2, 2\pi\}$, $i = 1, 2, 3$. Moreover, we may fix three parameters, e.g., $\phi_1 = \phi_2 = 0$ and $\theta_1 = 0$, owing to the invariance of the state ρ_3 under the collective $SU(2)$ rotation. Considering all the possible combinations of the remaining parameters p_{ij} , $ij = 12, 13, 23$ and $\theta_2, \theta_3, \phi_3$ from the set above, we found that $\text{Tr}(\rho_3\Pi) \geq 0$ is always true for the witness operators Π in (15). Therefore, genuine tripartite entanglement could not be witnessed by the general GHZ -type and W -type witnesses (15), as well.

Naturally, we may ask whether there exist other witnesses over the GHZ/W -types in (15) which are better suited for detecting GTE in the state ρ_3 . Indeed, in Ref. [23] it has been shown that there are several genuine tripartite entangled states which are not witnessed by the operators (15). Note, that nonlinear entanglement witnesses [24] may show improvement with respect to linear witnesses in the multipartite case as well. However, if we stick to linear functionals we are even able to reveal GTE in the state ρ_3 , as it will be discussed in the next subsection.

D. The witness operator of Gühne et al.

Gühne et al. [9] showed that the internal energy is a good indicator of genuine tripartite entanglement in macroscopic spin systems. The idea was to write the internal energy in terms of the mean value of the observables $W_{ijk} = \vec{\sigma}^i \cdot \vec{\sigma}^j + \vec{\sigma}^j \cdot \vec{\sigma}^k$, where $\vec{\sigma}^i = (\sigma_x^i, \sigma_y^i, \sigma_z^i)$ is the vector of Pauli spin operators associated with the qubit i , and the absolute value of $\langle W_{ijk} \rangle$ has been shown to be a witness itself, capable to detect GTE. Namely, it has been proven [9] that if the inequality

$$|\langle W_{ijk} \rangle| > 1 + \sqrt{5} \simeq 3.236 \quad (16)$$

holds, the qubits i, j, k are genuinely tripartite entangled.

Let us use this inequality (16) in order to reveal GTE in the degenerate Fermi gas among the spins of the three fermions i, j, k . Plugging the state ρ_3 in (2) into the expectation $\langle W_{ijk} \rangle = \text{Tr}(\rho_3 W_{ijk})$ one has $\langle W_{ijk} \rangle = 3(p_{ij} + p_{jk})$, which by substitution back into (16) gives the condition

$$|\langle W_{ijk} \rangle| := 3|p_{ij} + p_{jk}| > 1 + \sqrt{5} \quad (17)$$

for the existence of genuine tripartite entanglement in the degenerate Fermi gas. Next we discuss from the viewpoint of witnessed GTE by the mean of this condition two different three-fermion configurations:

(a) Consider the case investigated before in Section II B, that three particles lie evenly spaced on a line close to each other. Choosing $ijk = 123$ and recalling $p_{12} = p_{23} = 2/3$ from (11), by the virtue of (17), $|\langle W_{123} \rangle| = 4 > 1 + \sqrt{5}$, hence the three-fermion state ρ_3 corresponding to this arrangement of particles is genuine tripartite entangled.

(b) In this case the particles are separated from each other by equal distances, i.e., the particles are put on the vertices of an equilateral triangle. Owing to three-fold symmetry of this configuration the state ρ_3 contains an equal mixture of maximally entangled states $|\Psi^- \rangle$, that is, all p_{ij} , $ij = 12, 13, 23$ in (2) must have the same value. Further, considering the constraint $|p| = |p_{12} + p_{13} + p_{23}| \leq 1$ in (7) and also owing to the left-hand side of (17) we have $|\langle W_{123} \rangle| = |\langle W_{231} \rangle| = |\langle W_{132} \rangle| = 2|p| \leq 2$ implying that in this case all possible $|\langle W_{ijk} \rangle|$ (with different permutations of ijk) are smaller than the bound $1 + \sqrt{5}$. Consequently, no GTE can be revealed by the witness (16) of Gühne et al., no matter how far the fermions are separated from each other. It is reasonable to think that there is indeed no GTE associated with this highly symmetrical configuration, as it has been argued in Ref. [14] by attributing it to the Pauli principle. In the next section we construct from the observable W_{ijk} a witness operator \tilde{W}_{ijk} , which has a maximum eigenvalue smaller than unity ($\tilde{W}_{ijk} \leq \mathbb{I}_8$) and with the aid of it a lower bound is given for the amount of GTE in the state ρ_3 quantified by an entanglement monotone, the generalized robustness E_R .

III. DERIVING A LOWER BOUND TO THE GENERALIZED ROBUSTNESS E_R

Up to this point the observable W_{ijk} was applied for witnessing genuine tripartite entanglement. On the other, they are also good for quantifying it [16] (see [17] as an application to a magnetic material). The maximum eigenvalue of the operator $-W_{ijk}$ is 4, thus considering (16) we may construct the following witness operator,

$$\tilde{W}_{ijk} = \frac{(1 + \sqrt{5})\mathbb{I}_8 - W_{ijk}}{5 + \sqrt{5}}, \quad (18)$$

whose negative mean value $\text{Tr}(\rho \tilde{W}_{ijk})$ guarantees that the three-qubit state ρ is genuine tripartite entangled. Further the witness operator is normalized so that $\tilde{W}_{ijk} \leq \mathbb{I}_8$. It is apparent that provided the mean value $\langle W_{ijk} \rangle \geq 0$ for state ρ_3 (i.e., $p_{ij} + p_{jk} \geq 0$ according to calculations in Sec. II D), the witness operator (18) is just as powerful to detect GTE associated with state ρ_3 as $|\langle W_{ijk} \rangle|$ in the inequality (16).

The generalized robustness E_R as a GTE measure quantifies how robust the genuine tripartite entangled state ρ is under the influence of noise, and also has a geometrical meaning measuring the distance of ρ from the biseparable set B [25]. According to Ref. [16] E_R can be expressed in a Lagrange dual representation

$$E_R(\rho) = \max\{0, -\min_{\Pi \in M} \text{Tr}(\rho \Pi)\}, \quad (19)$$

where the set M is given by the restriction $\Pi \leq \mathbb{I}_8$ for the GTE witnesses Π .

Since \tilde{W}_{ijk} with any permutation of ijk defines a valid GTE witness with maximum eigenvalue smaller than unity, we are able to develop the lower bound

$$E_{R,\min}(\rho) = \max\{0, -\min_{ijk \in \{123, 231, 132\}} \text{Tr}(\rho \tilde{W}_{ijk})\} \quad (20)$$

to the generalized robustness (19) of an arbitrary state ρ on qubits 123, as it is discussed in Refs. [26, 27]. This lower bound by applying (18) for the particular state ρ_3 in (2) reads as

$$E_{R,\min}(\rho_3) = \max_{ijk \in \{123, 231, 132\}} \left\{0, \frac{3(p_{ij} + p_{jk}) - 1 - \sqrt{5}}{5 + \sqrt{5}}\right\}. \quad (21)$$

In the next section this formula will be applied to give explicitly a lower bound to the generalized robustness E_R of GTE for various configurations of three fermions, associated with the reduced state ρ_3 of the degenerate Fermi gas.

IV. NUMERICAL CALCULATIONS TO THE LOWER BOUND OF E_R

A. Fermion moving on a straight line

Now we concentrate on two different kinds of arrangements of the three fermions in the 3D degenerate Fermi gas, which configurations were also investigated in Ref. [14] from the viewpoint of bipartite entanglement shared between two arbitrary groups of three fermions.

(a) In the first instance a collinear arrangement is considered, namely we put three fermions on a straight line numbering them in the order 1, 2, and 3. The distance between particles 1 and 3 is r , and the intermediate particle 2 is by a distance of x away from particle 1 (shown by the geometrical picture of Fig. 1.(a)). In Fig. 1.(a), the lower bound to GTE quantified by E_R is plotted in the 3D Fermi gas according to the formula (21) in the function of x/r for different values $k_F r$ of the external fermions. The calculations can be in general performed only numerically, however for the limiting value $k_F r \rightarrow 0$ one obtains

$$\max_{ijk \in \{123, 231, 132\}} \{p_{ij} + p_{jk}\} = p_{12} + p_{23} = \frac{1}{1 - x/r + (x/r)^2}. \quad (22)$$

Substitution of this expression into (21) gives analytically the curve corresponding to $k_F r \rightarrow 0$. Note that formula (22) holds true independently of the dimensionality of the Fermi gas (i.e., both for the 2D and 3D cases). The curves produced in Fig. 1.(a) exhibit two essential features: For any given value of $k_F r$, the maximum of $E_{R,\min}$ is achieved by the symmetrical configuration (i.e., particle 2 is located at the midpoint of the line connecting particles 1 and 3), still presenting GTE in the system by the dimensionless distance $k_F r = 2.59$. On the other, when fermion 2 starting from this midpoint is moved toward fermion 1 in the case $k_F r \rightarrow 0$, the curve falls off to zero by the value $x/r = 1/2(1 - \sqrt{3(\sqrt{5} - 2)}) \simeq 0.08$. That is, if fermions 1 and 3 are a distance r away from each other and fermion 2 becomes closer than $x \simeq 0.08r$ to fermion 1 (or to fermion 3 in the symmetrically equivalent situation) formula (21) does not indicate GTE among the three fermions. This result fits to the monogamy property of entanglement [28], as in the case $x/r \rightarrow 0$ fermion 2 becomes maximally entangled with fermion 1, excluding the existence of any higher order entanglement in the system.

(b) Now let the three particles lie on the vertices of an isosceles triangle fermions 1 and 3 forming its base with length r , and fermion 2 is positioned by a distance of y from the midpoint of the base as it is illustrated in the geometrical part of Fig. 1.(b). The curves $E_{R,\min}$ in Fig. 1.(b) are plotted against y/r for different values of $k_F r$. As it can be observed, all the curves $E_{R,\min}$ plotted are monotonically decreasing in the function of the ratio y/r for any given $k_F r$. Similarly to case (a) the curve corresponding to $k_F r \rightarrow 0$ can be treated analytically, and one obtains vanishing GTE beyond the value $y/r = 1/2(\sqrt{3(\sqrt{5} - 2)}) \simeq 0.42$ (both in the 2D and 3D Fermi gases). This supports the result of case (b) in Sec. IID that three fermions located at the vertices of an equilateral triangle (where $y/r = \sqrt{3}/2 \simeq 0.866$) are not genuine tripartite entangled independent of the separation distance r . It is also apparent from Fig. 1.(b) that for a fixed ratio y/r , $E_{R,\min}$ is maximal when $k_F r \rightarrow 0$, for in this case the antisymmetrization effect between the three particular fermions and the rest of the fermions (which reduces the amount of quantum correlations shared among the three fermions) becomes negligible.

B. Fermion moving in a plane

We now turn to the situation (pictured in the geometrical part of Fig. 2) when fermion 2 is allowed to move in the two-dimensional plane given by polar coordinates (θ, q) with an origin at the midpoint of the line of length r connecting fermion 1 and fermion 3. Let us restrict fermion 2 to be positioned within the circle with radius $r/2$. Recalling the definition of the GTE distance from Sec. I, in this case the GTE distance is equal to the maximum separation length r between the two external

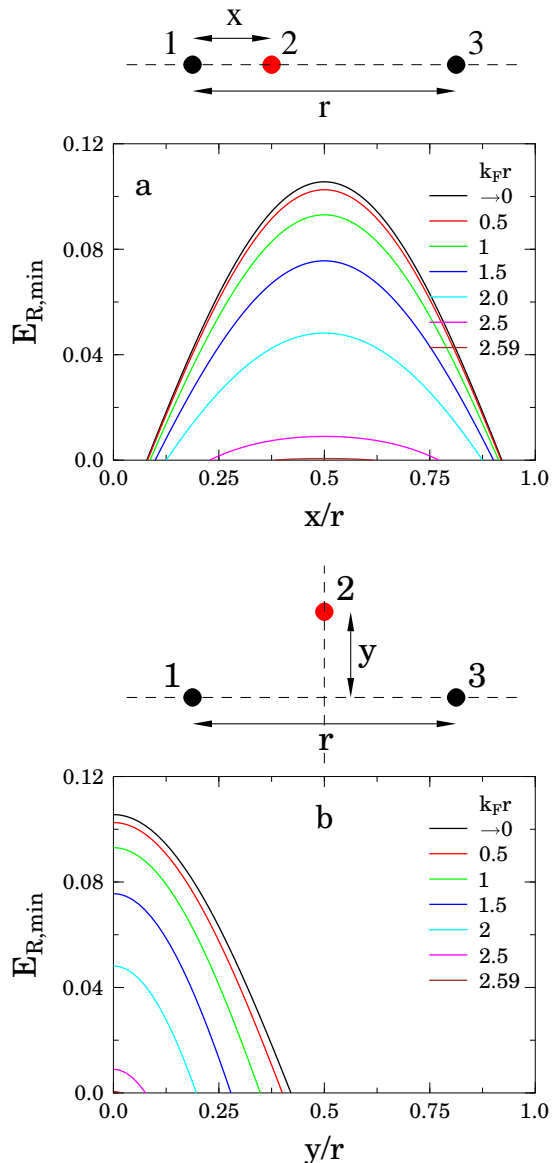


FIG. 1: (color online) Lower bound to the generalized robustness E_R of genuine tripartite entanglement shared by three fermions is plotted for the 3D Fermi gas for the cases (a) fermion 2 is moved away from the position of fermion 1 toward the position of fermion 3, (b) fermion 2 is moved away from the midpoint of the line connecting fermion 1 and fermion 3 normal to this line (see the respective schematic geometrical pictures). The curves are plotted in both cases for the following dimensionless distances between fermion 1 and fermion 3: $k_F r \rightarrow 0$ (displayed in black) and $k_F r = 0.5, 1, 1.5, 2, 2.5, 2.59$ (displayed in color).

fermions, below which the three fermions are genuine tripartite entangled.

In what follows, we inquire the shape of region within particle 2 could be located so that fermions 1, 2, and 3 by a fixed relative distance r would be genuine tripartite entangled. Further, owing to the symmetry of the configuration it suffices to study the interval $\theta \in [0, \pi/2]$, i.e.,

particle 2 is restricted to be situated on a quarter-disk of radius $r/2$. The polar plot of Fig. 2 represents curves which distinguish regions with (left side) and without (right side) witnessed GTE in the system, by the following values of the dimensionless distances $k_F r \rightarrow 0$ and $k_F r = 1, 2, 2.5, 2.59$. The witnessed GTE (i.e., to decide whether $E_{R,\min}(\rho_3) > 0$) corresponding to these curves for the various values of $k_F r$ was calculated according to the formula (21).

The case $k_F r \rightarrow 0$ can be treated analytically yielding the result (as it can be read off from Fig. 2) that by $k_F r \rightarrow 0$ GTE is present in the system provided fermion 2 is located inside a disk with radius $q \simeq 0.42r$ (generalizing the results $x \simeq 0.08r$ and $y \simeq 0.42r$ in the limit $k_F r \rightarrow 0$ obtained in Sec. IV A). Now one can see from the shape of the polar curves that for greater $k_F r$ the corresponding disk associated with GTE squeezes toward the axis of particles 1 and 3, eventually contracting on the origin $q = 0$. It is noted that the same behavior would have been observed for the case of 2D Fermi gas, as well. This implies that if in this particular case we were searching for the GTE distance (i.e., the maximum separation r , below which GTE exists) then we should focus on the case where particle 2 is located at the midpoint between particles 1 and 3. This task will be performed in the sequel both for the 2D and 3D degenerate Fermi gases.

V. AN UPPER AND A LOWER BOUND TO THE GTE DISTANCE IN THE 2D AND 3D DEGENERATE FERMI GASES

A. Lower bound

In the present section the three-fermion configuration is investigated, where the particles 1, 2 and 3 are positioned evenly spaced on a straight line, with a relative distance r between the external particles 1 and 3. We develop both for the 2D and 3D Fermi gases an upper and a lower bound to the relative distance r , beyond which GTE disappears.

Let us first calculate numerically and plot the lower bound to the generalized robustness of GTE defined by (21) in the function of $k_F r$. In Fig. 3 the respective curves are plotted both for the two- and three-dimensional degenerate Fermi gases, and numerics shows that $E_{R,\min}(\rho_3)$ vanishes beyond, i.e., the lower bound to the GTE distance is

$$\begin{aligned} r_{\min}^{2D} &= 2.3588/k_F, \\ r_{\min}^{3D} &= 2.5964/k_F, \end{aligned} \quad (23)$$

respectively. Let us compare these values (23) with the bipartite entanglement distance (i.e., the maximal separation distance between two entangled fermions), which are slightly smaller, and are given explicitly by the values [14] $1.6163/k_F$ and $1.8148/k_F$ for the 2D and 3D Fermi gases, respectively.

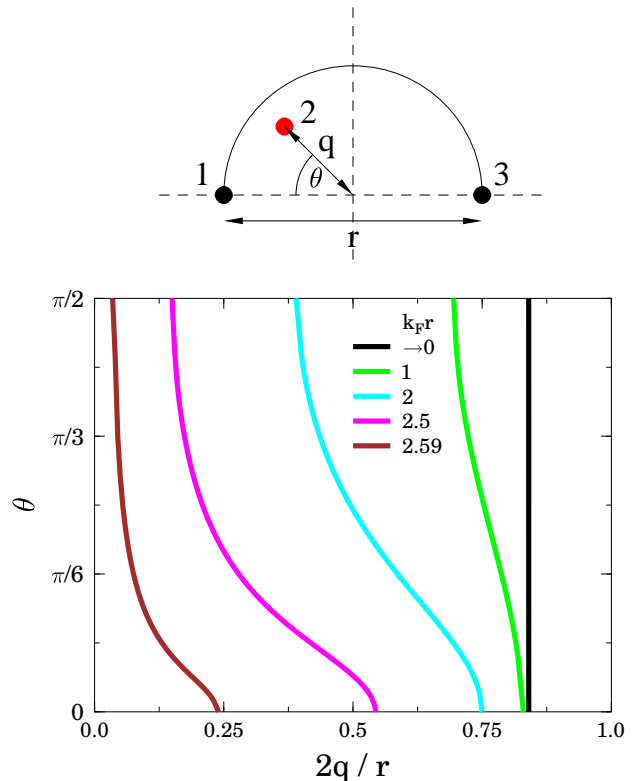


FIG. 2: (color online) Witnessed genuine tripartite entanglement among three fermions is plotted for the 3D Fermi gas for the configuration where fermion 2 (with polar coordinates (θ, q)) is allowed to move in a disk of radius $r/2$ centered at the midpoint between fermion 1 and fermion 3, as shown by the geometrical picture. The polar plot represents curves with black, green, cyan, magenta and brown colors, which separate the regions associated with GTE (left-hand side) from regions without having GTE (right-hand side) for values of the dimensionless distances $k_F r \rightarrow 0$, $k_F r = 1, 2, 2.5, 2.59$, respectively.

For the 3D Fermi gas the p_{ij} parameters of the state ρ_3 corresponding to r_{\min}^{3D} are

$$p_{12} = p_{23} = 0.539345, \quad p_{13} = -0.160702. \quad (24)$$

We can also observe in Fig. 3, as one may expect, that the curves are monotonically decreasing, such as in the bipartite case for the entanglement measure negativity [14].

B. Upper bound

We continue with studying the particular three-fermion configuration discussed in the previous subsection in order to establish an upper bound to the GTE distance, beside the lower bound already obtained. Exploiting the mirror symmetry of the configuration, for any given distance r between the positions of particle 1 and particle 3 we have $p_{12} = p_{23}$, thus in this case parameters r_k defined by (6) in Section II A can be expressed

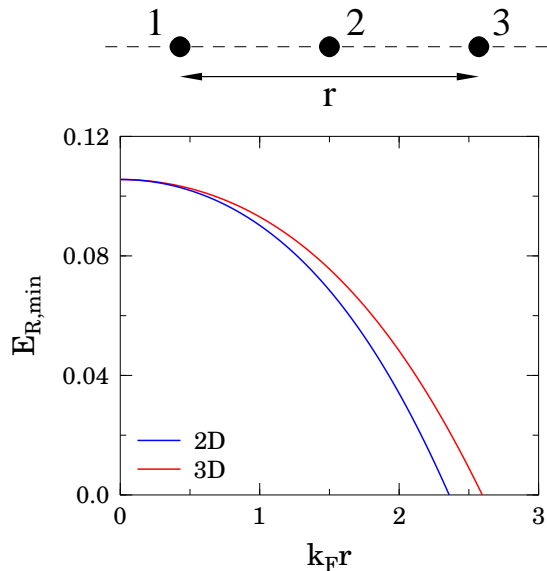


FIG. 3: (color online) Lower bound to the generalized robustness E_R of genuine tripartite entanglement is plotted both for the two- and three-dimensional degenerate Fermi gases in the function of the dimensionless distance $k_F r$, where r is the relative distance between the positions of fermion 1 and fermion 3, and fermion 2 is located at the midpoint, as shown by the upper part of the figure.

through p_{12} and p_{13} alone, and we obtain the relation

$$r_2 = \sqrt{3}r_1. \quad (25)$$

On the other, by applying Theorem 7 of Eggeling and Werner [20] it is asserted that a three-qubit state is biseparable with respect to the partition 1|23 if the following inequalities are satisfied:

$$\begin{aligned} -1 < r_1 - 2r_+ < 0, \\ 3r_2^2 + 3r_3^2 + (1 - 3r_+)^2 \leq (r_1 - 2r_+)^2. \end{aligned} \quad (26)$$

Now let us calculate the boundary of the area in the plane (r_1, r_2) described by these inequalities (26) by $r_+ = 0.041$ and $r_3 = 0$, which parameters correspond to the symmetrical configuration of separation r_{\min}^{3D} between fermion 1 and fermion 3 with parameters (24). The solution of the inequality (26) by $r_+ = 0.041$, $r_3 = 0$ corresponds to the leftmost yellow shaded semi-disk in Fig. 4, representing states in the section $r_+ = 0.041$ and $r_3 = 0$ that are separable with respect to the partition 1|23. The other two disks (representing biseparable states with respect to partitions 12|3, 13|2) can be obtained through $\pm 2\pi/3$ rotations around the origin of the plane (r_1, r_2) [29] owing to the permutation symmetry of the three subsystems. The boundary of the convex hull of these semi-disks are indicated by solid blue line segments in Fig. 4. All the three-qubit states in the section $r_+ = 0.041$ and $r_3 = 0$ which lie inside this polygon are in the class of biseparable states B . However, since this area corresponds to a section, biseparable states in this section may exist outside the polygon as well.

Next let us determine the explicit position of the point corresponding to the mirror-symmetrical configuration with separation r_{\min}^{3D} between the two external fermions. In this particular symmetrical configuration according to (25) the ratio $r_2/r_1 = \sqrt{3}$ and we also have $r_1 = (p_{13} - p_{12})/2$. The above ratio has been displayed in Fig. 4 by a dashed line and the point on this line with coordinate $r_1 = -0.35$ (obtained by plugging the values (24) into the above formula for r_1) corresponding to the separation r_{\min}^{3D} with $E_{R,\min} = 0$ has been designated by the red cross marker. Numerics shows, that this point lies outside the solid blue polygon, as it ought to owing to $E_R \geq 0$ associated with the point. By inspection, on the other, this point is very close to the border of the polygon.

Indeed, explicit numerical calculations yield that the distance r between the two outer fermions corresponding to the border of the polygon is $r_{\max}^{3D} = 2.5988/k_F$. This value was obtained by tuning the value of r_+ from 0.041 up to $\simeq 0.0415$ by the mean of increasing the separation r starting from the value r_{\min}^{3D} so that by r_{\max}^{3D} the point represented by the the cross marker would lie just on the edge of the polygon. However, this distance $r_{\max}^{3D} = 2.5988/k_F$ is just an upper bound to the GTE distance for the 3D Fermi gas. On the other, similar evaluations give the value $r_{\max}^{2D} = 2.3599/k_F$ for the 2D Fermi gas. Comparing these values with the ones in (23) corresponding to the lower bound, it shows that the upper and lower bounds to the GTE distance are indeed very close to each other both for the 2D and 3D Fermi gases. Hence, this implies that the witness of Gühne et al. [9] in our particular problem ought to be close to an optimal one.

VI. DISCUSSION

Previous works (e.g., [13, 14]) explored that bipartite entanglement exists within the order of the Fermi wavelength $1/k_F$ at zero temperature in the non-interacting Fermi gas and may even persist for nonzero temperatures (e.g., [19, 30]). Since the system consists of non-interacting fermions, entanglement is purely due to particle statistics and not to any physical interaction between the particles. In the present work we found the result as an extension of the formerly studied bipartite case that particle statistics is capable to generate genuine tripartite entanglement (GTE) as well. Furthermore, it has been found that the diameter of the three-fermion configuration wherein GTE is present (a lower bound to the maximum diameter is given explicitly by (23)) is comparable with the maximum relative distance between two entangled fermions, both in the 2D and 3D Fermi gases. Looking at higher order entanglement as a useful resource, the presence of GTE in Fermi systems would be promising to allow for performing new quantum information processing tasks, exemplified by the *GHZ* paradox [2]. However, in order to do so, the amount of entanglement

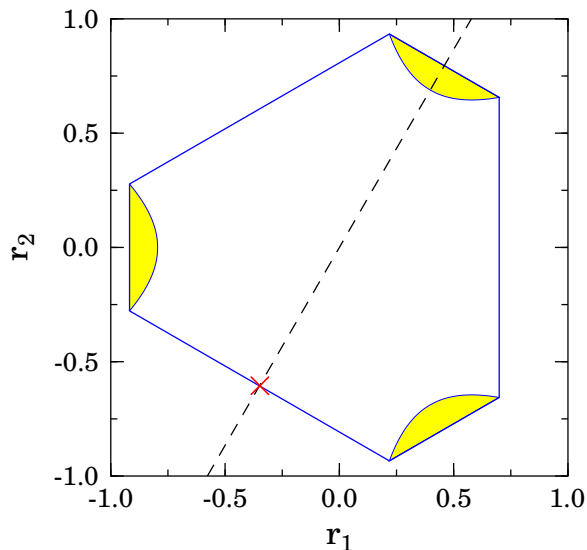


FIG. 4: (color online). The three yellow shaded half-disks represent areas corresponding to biseparable states with respect to the partitions 1|23, 12|3 and 13|2 on the (r_1, r_2) plane by the section $r_+ = 0.041$ and $r_3 = 0$ for the 3D Fermi gas. The solid blue straight lines bound the set of biseparable states B at this particular section. The equation $r_2 = \sqrt{3}r_1$ is represented by the dashed line, and the red cross stands for the point which is located on this line with coordinate $r_1 = -0.35$.

stored by three fermions should be somehow extracted from the system. In the present article, though, we did not consider this problem some explicit schemes has been put forward recently in the bipartite setting [31, 32, 33], some of which might be extended to the tripartite setting as well.

Namely, in Ref. [31] it has been shown that bipartite entanglement can exist between non-interacting fermions on a lattice and can extend over multiple lattice sites even if the entanglement is quantified by the most restrictive measure, the entanglement of particles [34]. Further, considering that in the continuum limit the entanglement of particles corresponds to the entanglement in the spin reduced density matrix [31], by continuity arguments genuine tripartite entanglement, quantified by the measure

entanglement of particles, should exist in the lattice system as well. Thus, in the near future optical lattice implementations may offer a simulation technique to observe the phenomenon of genuine tripartite entanglement among non-interacting fermions in a lattice.

On the other, in the continuum limit the extraction of genuine tripartite entangled particles seems to be a more difficult problem: As it has been shown [13] the entanglement distance between two fermions is inversely proportional to the Fermi momentum k_F , and k_F^3 in turn is proportional to the density of particles. In the case of conduction electrons in a usual metal the density is very large indicating an entanglement distance of the order of a few angstroms. This failure might be avoided by using 2D electron gas formed in GaAs heterostructure, where the entanglement distance is in the order of hundred angstroms [19] or using stored ultra-cold neutrons in a carefully devised experiment [33]. Also, note the intriguing proposal, exploiting decoherence effects to extract bipartite entanglement created merely by particle statistics from semiconductor quantum wells [32]. Although the GTE distance in (23) is comparable (even greater) than the bipartite entanglement distance both for the 2D and 3D Fermi gases, technically these proposals appear to be very demanding when applied to the three-party setting.

Finally, we would like to mention interesting future directions as a continuation of the present work. One could for example apply the same methods as in the present article for determining GTE distance in Fermi gases trapped in a harmonic trap [35] or considering GTE not only in spin, but in other internal degrees of freedom as well [36]. Also the possible existence of genuine multipartite entanglement beyond the three-party scenario remains to be explored.

Acknowledgments

This work was supported by the Grant Öveges of the National Office for Research and Technology.

-
- [1] M.A. Nielsen and I.L. Chuang, *Quantum Computation and Quantum Information*, (Cambridge University Press, 2000).
 - [2] D.M. Greenberger, M.A. Horne, A. Shimony, A. Zeilinger, *Am. J. Phys.* **58** 1131 (1990).
 - [3] R. Raussendorf and H.J. Briegel, *Phys. Rev. Lett.* **86** 5188 (2001).
 - [4] V. Giovannetti, S. Lloyd, L. Maccone, *Science* **306** 1330 (2004).
 - [5] S.D. Bartlett, T. Rudolph, and R.W. Spekkens, *Phys. Rev. Lett.* **91** 027901 (2003).
 - [6] Z. Zhao, Y.-A. Chen, A.-N. Zhang, T. Yang, H.J. Briegel, and J.-W. Pan, *Nature* **430** 54 (2004).
 - [7] A. Acín, D. Bruß, M. Lewenstein, and A. Sanpera, *Phys. Rev. Lett.* **87** 040401 (2001).
 - [8] M.B. Plenio, S. Virmani, *Quant. Inf. Comp.* **7** 1 (2007).
 - [9] O. Gühne, G. Tóth, and H.J. Briegel, *New. J. Phys.* **7** 229 (2005).
 - [10] T.J. Osborne and M.A. Nielsen, *Phys. Rev. A* **66** 032110 (2002).
 - [11] T.R. de Oliveira, G. Rigolin, M.C. de Oliveira, E. Miranda, *Phys. Rev. Lett.* **97** 170401 (2006).
 - [12] V. Vedral, *New J. Phys.* **6** 102 (2004).
 - [13] V. Vedral, *Cent. Eur. J. Phys.* **1** 289 (2003).

- [14] C. Lunkes, Č. Brukner, and V. Vedral, Phys. Rev. Lett. **95** 030503 (2005).
- [15] G. Tóth and O. Gühne, Appl. Phys. B **82** 237 (2006).
- [16] F.G.S.L. Brandão, Phys. Rev. A **72** 022310 (2005).
- [17] T.G. Rappoport, L. Ghivelder, J.C. Fernandes, R.B. Guimarães, M.A. Continentino, ArXiv: quant-ph/0608403.
- [18] D. Cavalcanti, M. França Santos, M.O. Terra Cunha, C. Lunkes, V. Vedral, Phys. Rev. A. **72** 062307 (2005).
- [19] S. Oh and J. Kim, Phys. Rev. A. **69** 054305 (2004).
- [20] T. Eggeling and R.F. Werner, Phys. Rev. A. **63** 042111 (2001).
- [21] B.M. Terhal, Phys. Lett. A **271** 319 (2000).
- [22] M. Bourennane, M. Eibl, C. Kurtsiefer, S. Gaertner, H. Weinfurter, O. Gühne, P. Hyllus, D. Bruß, M. Lewenstein, and A. Sanpera, Phys. Rev. Lett. **92** 087902 (2004).
- [23] D. Cavalcanti and M.O. Terra Cunha, ArXiv: quant-ph/0506035.
- [24] O. Gühne, N. Lütkenhaus, ArXiv: quant-ph/0612108.
- [25] D. Cavalcanti, F.G.S.L. Brandão, and M.O. Terra Cunha, ArXiv: quant-ph/0510068.
- [26] D. Cavalcanti and M.O. Terra Cunha, Appl. Phys. Lett. **89** 084102 (2006).
- [27] J. Eisert, F.G.S.L. Brandão, and K.M.R. Audenart, ArXiv: quant-ph/0607167.
- [28] V. Coffman, J. Kundu, and W.K. Wootters, Phys. Rev. A **61** 052306 (2000).
- [29] G. Tóth and A. Acín, Phys. Rev. A **74** 030306(R) (2006).
- [30] C. Lunkes, Č. Brukner, and V. Vedral, Phys. Rev. A **71** 034309 (2005).
- [31] M.R. Dowling, A.C. Doherty, H.M. Wiseman, Phys. Rev. A. **73** 052323 (2006).
- [32] D. Cavalcanti, L.M. Moreira, F. Matinaga, M.O. Terra Cunha, M. França Santos, ArXiv: quant-ph/0608141.
- [33] M.O. Terra Cunha and V. Vedral, ArXiv: quant-ph/0607224.
- [34] H.M. Wiseman and J.A. Vaccaro, Phys. Rev. Lett. **91** 097902 (2003).
- [35] X.X. Yi, Eur. J. Phys. D **39** 465 (2006).
- [36] D.-M. Chen, W.-H. Wang, and L.-J. Zou, ArXiv: cond-mat/0605378.